1,3-Dipolar Cycloaddition to the Fe−O=C Fragment. 19. Synthesis and Properties of $Fe(CO)_2(PR_3)(R^1N{=}C(R^2){-}C(R^3){=}O)$ and $Fe(CO)(Ph_2PCH_2CH_2PPh_2)(R^1N{=}C(R^2){-}C(R^3){=}O)$ and Their Reactivity toward Dipolarophiles. First X-ray Crystal Structure of the Initial Bicyclo[2.2.1] Adduct

Ron Siebenlist, Hans-Werner Frühauf,*,† and Kees Vrieze

University of Amsterdam, Institute of Molecular Chemistry, Nieuwe Achtergracht 166, 1018 WV Amsterdam, The Netherlands

Wilberth J. J. Smeets and Anthony L. Spek

Bijvoet Center for Biomolecular Research, Crystal and Structural Chemistry, Utrecht University, Padualaan 8, 3584 CH Utrecht, The Netherlands

Received July 24, 2002

Complexes **7ak**−**an**, **7bk**,**bm** [$(R^1N{=}C(R^2){-}C(R^3){=}O)Fe(CO)_2PR_3$ **a**: $R^1 = {}^t$Bu, R^2 = H, R^3 = Ph; **b**: R^1 = Me, R^2 = Ph, R^3 = Ph; **k**: R = OMe; **l**: R = Ph; **m**: R = Et; **n**: R = ^{n}Pr], and **7ao**,**bo** [$(R^1N{=}C(R^2){-}C(R^3){=}O)Fe(CO)Ph_2PCH_2CH_2PPh_2$] have been prepared by substitution of CO in the respective tricarbonyl complexes **1a**,**b** at room temperature. Various dynamic processes have been investigated by ^{13}C and ^{31}P NMR. On the IR time scale, complex **7bk** exists in two distinct isomeric forms. Complexes **7** have been characterized by IR, UV−vis, and ^{1}H, ^{13}C, and ^{31}P NMR spectroscopy. Surprisingly, in the 1,3-dipolar cycloaddition reaction of complexes **7** with the dipolarophiles dimethyl acetylenedicarboxylate (DMAD, **v**), methyl propynoate (**w**), phenyl acetylene (**x**), and *p*-methoxyphenyl-isothiocyanate (**y**) the bicyclic ferra[2.2.1] complexes **8**, i.e., the initial cycloadducts, are stable and isolable. With dimethyl maleate (**z**) it is formed reversibly. Complexes **8** containing one phosphorus ligand are formed as two non-interconverting isomers. The molecular structure of **8aov**, $C_{45}H_{45}FeNO_6P_2$, has been determined by single-crystal X-ray diffraction. In pentane, the initial cycloadduct (**8bv**) of the tricarbonyl **1b** with DMAD is insoluble and precipitates. In solution above −30 °C **8bv** reacts further by insertion of CO into the Fe−O bond to the $Fe(CO)_3$(butenolide) complex **10bv**. No intermediates can be detected by ^{1}H, ^{13}C, and IR monitoring. The other complexes **8** do not insert CO and slowly decompose on stirring at room temperature in THF. From the decomposition of complexes **8** with α-iminoketone **a**, the organic compound **11a** can be isolated. The cycloaddition reaction of **1a** with DMAD (**v**) in the presence of PR_3 (**k**: R = OMe; **l**: R = Ph) results without detectable intermediates in the formation of the $Fe(CO)_2PR_3$(butenolide) complexes **10akv**,**alv.** They are formed as three and two non-interconverting isomers, respectively. Reaction of **8bv** with PEt_3 also results in the formation of the butenolide complex **10bmv**; however, here the PEt_3 ligand occupies exclusively one of the equatorial positions. An explanation for the isomeric ratios of complexes **8** and **10** is discussed.

Introduction

In the previous parts of this series we have reported on the reactions of $M(CO)_{3-n}(CNR)_n(R^1\text{-DAB})$[1] (M = Fe, Ru; n = 0, 1, and 3) and $Fe(CO)_3(R^1N{=}C(R^2)\text{-}C(R^3){=}O)$ complexes (**1**) with unsaturated substrates, e.g., activated alkynes,[2−7] alkenes,[8,9] and isothiocyanates,[10−12] resulting in synthetically interesting coordinated heterocycles such as in complexes **4** and **5** (cf. Scheme 1).

The initial step in these reactions consists of an oxidative 1,3-dipolar cycloaddition of the activated alkyne (the dipolarophile) across the M−X=C fragment (the 1,3-dipole), which results in the formation of the

† E-mail: hwf@science.uva.nl. Fax: +31-20-525 6456.

(1) The abbreviations used throughout this text are as follows: R^1-DAB: 1,4-diaza-1,3-butadienes of formula $R^1{-}N{=}C(H){-}C(H){=}N{-}R^1$; DMAD: dimethyl acetylenedicarboxylate; MP: methyl propynoate; DMM: dimethyl maleate; DPPE: 1,2-bis(diphenylphosphanyl)ethane.

(2) Frühauf, H.-W.; Seils, F.; Romão, M. J.; Goddard, R. J. *Angew. Chem.* **1983**, *95*, 1014−16; *Angew. Chem., Int. Ed. Engl.* **1983**, *22*, 992; *Angew. Chem. Suppl.* **1983**, 1435.

(3) de Lange, P. P. M.; Frühauf, H.-W.; Kraakman, M. J. A.; van Wijnkoop, M.; Kranenburg, M.; Groot, A. H. J. P.; Vrieze, K.; Fraanje, J.; Wang, Y.; Numan, M. *Organometallics* **1993**, *12*, 417−427.

(4) de Lange, P. P. M.; van Wijnkoop, M.; Frühauf, H.-W.; Vrieze, K.; Goubitz, K. *Organometallics* **1993**, *12*, 428−439.

(5) van Wijnkoop, M.; Siebenlist, R.; de Lange, P. P. M.; Frühauf, H.-W.; Vrieze, K.; Smeets, W. J. J.; Spek, A. L. *Organometallics* **1993**, *12*, 4172−4181.

10.1021/om020605z CCC: $22.00
Publication on Web 11/07/2002

Scheme 1. Reactions of $Fe(CO)_2L(R^1\text{-DAB})$ and $Fe(CO)_3$(α-iminoketone) with Electron-Deficient Alkynes

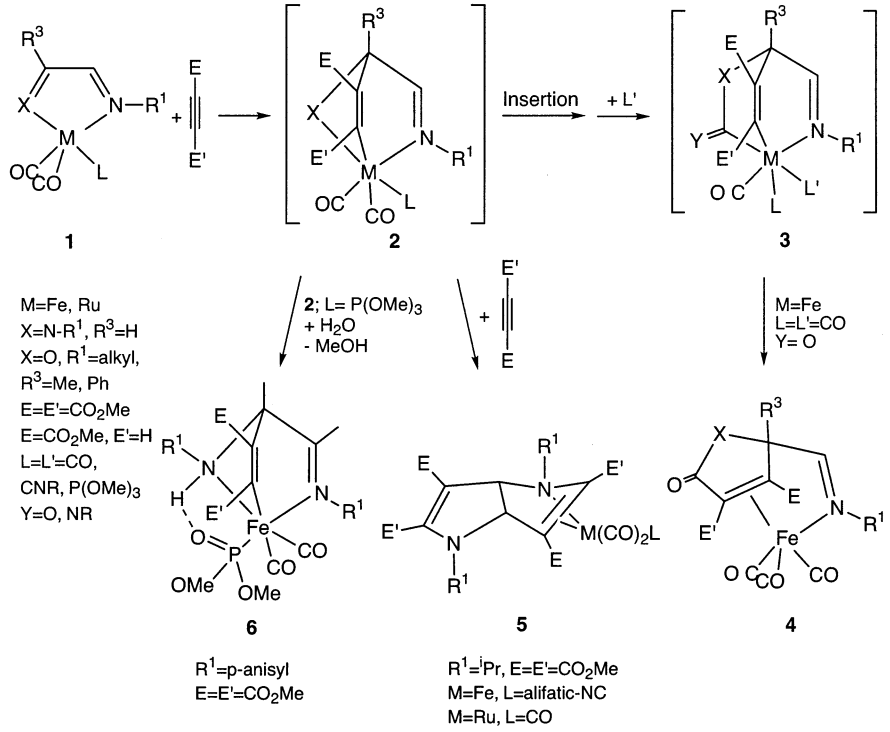

bicyclo[2.2.1] intermediate **2**. The subsequent reaction of this intermediate and accordingly the product formation depend on the co-ligand L, the additional ligand L′, the metal M, and the nature of the 1,4-dihetero-1,3-butadiene system. In case of R^1-DAB (X = NR^1), this mechanism is firmly supported by the isolation and characterization of the N-protonated ferrabicyclo[2.2.1] complex[13] (**6**) and the isostructural N-protonated bicyclo-[2.2.1]$Ru(CO)_3^+[BF_4^-]$ complex,[7] which both closely resemble intermediate **2**, as well as by the formation of the $M(CO)_2(L)$(THPP) complexes (**5**). In the case of iron, the bicyclo[2.2.2] complex **3** formed upon insertion of CO into the Fe−N bond and uptake of an additional ligand L′ is thermally labile when L = L′ = CO and rearranges, via reductive elimination, to the $Fe(CO)_3$(pyrrolinone) complex **4**. When a more σ-donating/less π-accepting ligand than CO is used as co-ligand L or as additional ligand L′, e.g., CNR or $P(OMe)_3$, the bicyclo[2.2.2] complex **3** is stable. The stabilizing effect has been attributed to the strengthening of the Fe−C bond *trans* to the σ-donor ligand, i.e., reinforcement of one of the bonds that is broken in the rearrangement giving complex **4**.[14]

Reaction of the closely related $Fe(CO)_3(R^1N{=}C(R^2){-}C(R^3){=}O)$ (R^3 = Me, Ph) complexes showed that these complexes exhibit similar reactivity (cf. Scheme 1, X = O),[5,6] whereby the 1,3-dipolar cycloaddition proceeds regioselective exclusively over the Fe−O═C fragment with formation of the $Fe(CO)_3$(butenolide) complexes **4**. As opposed to the analogous reactions of $M(CO)_3(R^1\text{-DAB})$, intermediates **2** and **3** have not been observed in this reaction even at very low temperature. Therefore the reaction mechanism is based on the analogy with the reactions of $M(CO)_3(R^1\text{-DAB})$ (M = Fe, Ru). The stabilizing effect of σ-donor ligands on the bicyclo[2.2.2] complex **3** prompted us to synthesize the $Fe(CO)_2(PR_3)$-$(R^1N{=}C(R^2){-}C(R^3){=}O)$ (R = OMe, Ph, Et, ^{n}Pr) and Fe-(CO)(DPPE)$(R^1N{=}C(R^2){-}C(R^3){=}O)$ (DPPE = 1,2-bis-(diphenylphosphino)ethane) complexes and study their 1,3-dipolar reactivity. Second, PR_3 can be used as additional ligand. The objective was to see if we could stabilize intermediates **2** and **3** in this way and (spectroscopically) characterize them. Furthermore, the substitution of CO for the better σ-donating/less π-accepting phosphorus ligands was expected to lead to an enhanced 1,3-dipolar reactivity. Analogously, substitution of CO for the better σ-donating/less π-accepting CNR ligands in $Fe(CO)_3(R^1\text{-DAB})$ resulted in the highly activated Fe-$(CNR)_3(R^1\text{-DAB})$ complexes, which also react with less activated dipolarophiles such as alkenes[9] and hetero-allenes,[10−12] resulting in complexes analogous to **3**.

In the present paper we report on the synthesis and properties of the $Fe(CO)_2(PR_3)(R^1N{=}C(R^2){-}C(R^3){=}O)$ and Fe(CO)(DPPE)$(R^1N{=}C(R^2){-}C(R^3){=}O)$ complexes (**7**). The 1,3-dipolar cycloaddition reaction of complexes **7** and $Fe(CO)_3(MeN{=}C(Ph){-}C(Ph){=}O)$ (**1b**) with DMAD[1] and some other dipolarophiles are studied. Also the reactions of $Fe(CO)_3(^tBuN{=}C(H){-}C(Ph){=}O)$ (**1a**) with

(6) van Wijnkoop, M.; Siebenlist, R.; Ernsting, J. M.; de Lange, P. P. M.; Frühauf, H.-W.; Horn, E.; Spek, A. L. *J. Organomet. Chem.* **1994**, *482*, 99−109.
(7) van Wijnkoop, M.; de Lange, P. P. M.; Frühauf, H.-W.; Vrieze, K.; Wang, Y.; Goubitz, K.; Stam, C. H. *Organometallics* **1992**, *11*, 3607−3617.
(8) van Wijnkoop, M.; de Lange, P. P. M.; Frühauf, H.-W.; Vrieze, K.; Smeets, W. J. J.; Spek, A. L. *Organometallics* **1995**, *14*, 4781−4791.
(9) de Lange, P. P. M.; de Boer, R. P.; van Wijnkoop, M.; Ernsting, J. M.; Frühauf, H.-W.; Vrieze, K.; Smeets, W. J. J.; Spek, A. L.; Goubitz, K. *Organometallics* **1993**, *12*, 440−453.
(10) de Lange, P. P. M.; Alberts, E.; van Wijnkoop, M.; Frühauf, H.-W.; Vrieze, K.; Kooijman, H.; Spek, A. L. *J. Organomet. Chem.* **1994**, *465*, 241−249.
(11) Feiken, N.; Frühauf, H.-W.; Vrieze, K.; Fraanje, J.; Goubitz, K. *Organometallics* **1994**, *13*, 2825−2832.
(12) Feiken, N.; Frühauf, H.-W.; Vrieze, K.; Veldman, N.; Spek, A. L. *J. Organomet. Chem.* **1996**, *511*, 281−291.
(13) Frühauf, H.-W.; Seils, F.; Stam, C. H. *Organometallics* **1989**, *8*, 2338−2343.
(14) Frühauf, H.-W.; Seils, F. J. *J. Organomet. Chem.* **1987**, *323*, 67−76.

DMAD in the presence of PR_3 and of the bicyclo[2.2.1]-$Fe(CO)_3$ complex **8bv** in the presence of PEt_3 are studied.

Experimental Section

Materials and Apparatus. ^1H and ^{13}C NMR spectra were recorded on a Bruker AMX-300 spectrometer. The IR spectra were recorded on a Biorad FTIR-7 spectrophotometer. Elemental analyses were carried out by Dornis & Kolbe, Microanalytisches Laboratorium, Mülheim a. d. Ruhr, Germany. The solvents were carefully dried and distilled under nitrogen prior to use. All preparations were carried out under an atmosphere of dry nitrogen by conventional Schlenk techniques. Silica gel for column chromatography (Kieselgel 60, 70−230 mesh, E. Merck, Darmstadt, Germany) was dried and activated prior to use by heating to 180 °C under vacuum for 16 h. $Fe(CO)_5$ (Strem Chemicals), $P(OMe)_3$ (**k**), PPh_3 (**l**), PEt_3 (**m**), $P(^nPr)_3$ (**n**), and DPPE (**o**) were used as commercially obtained. $Fe_2(CO)_9$[15] and the starting complexes $Fe(CO)_3(R^1N{=}C(R^2){-}C(R^3){=}O)$ ($R^1 = {}^t$Bu, R^2 = H, R^3 = Ph (**1a**); R^1 = Me, R^2 = Ph, R^3 = Ph (**1b**)) were prepared according to published procedures.[5,16]

Synthesis of $Fe(CO)_2(PR_3)(R^1N{=}C(R^2){-}C(R^3){=}O)$ (7ak−n, 7bk,bm) (with PR_3 = $P(OMe)_3$ (k), PEt_3 (m), $P(^nPr)_3$ (n)). To a solution of the appropriate $Fe(CO)_3(R^1N{=}C(R^2){-}C(R^3){=}O)$ (**1**) (1.00 mmol) in 30 mL of pentane was added 1.1 equiv of the respective PR_3. The reaction was followed by IR spectroscopy. For PEt_3 and $P(^nPr)_3$ complete conversion of the starting complex took approximately 10 min. During the reaction the color changed from dark purple to dark black-purple. For $P(OMe)_3$ complete conversion took approximately 16 h, during which time the color of the solution hardly changed. When the reaction was carried out with 2 equiv of $P(OMe)_3$, the reaction time was reduced to 4 h and almost no (<5%) disubstitution was observed. The obtained solutions were used for further reactions, assuming a quantitative formation of **7ak**−**n** and **7bk**,**bm**.

Synthesis of $Fe(CO)_2(PPh_3)({}^t$BuN=C(H)−C(Ph)=O) (7al). To a solution of $Fe(CO)_3({}^t$BuN=C(H)−C(Ph)=O) (**1a**) (1.00 mmol) in 20 mL of pentane and 10 mL of THF was added 1.1 equiv of PPh_3. The reaction was followed by IR spectroscopy and revealed that complete conversion took 36 h. During the reaction the color of the solution became black-purple. Addition of 2 equiv of PPh_3 reduced the reaction time to 12 h, and formation of the disubstituted product was not observed. The obtained solution was used for further reactions, assuming a quantitative formation of **7al**.

Synthesis of $Fe(CO)(DPPE)(R^1N{=}C(R^2){-}C(R^3){=}O)$ (7ao,bo). To a solution of the appropriate $Fe(CO)_3(R^1N{=}C(R^2){-}C(R^3){=}O)$ (**1**) (1.00 mmol) in 20 mL of pentane and 10 mL of THF was added 1.1 equiv of DPPE. The reaction was followed by IR spectroscopy and revealed a complete conversion of the starting complex to the intensely blue **7ao** and purple-blue **7bo**, respectively, within 5 h. The obtained solutions were directly used for further reactions, assuming a quantitative formation of **7ao**,**bo**.

NMR Samples of $Fe(CO)(DPPE)(R^1N{=}C(R^2){-}C(R^3){=}O)$ (7ao,bo). The NMR samples of **7ao**,**bo** obtained from the reaction mixture (see above) were paramagnetic, which made characterization by NMR difficult. Therefore the NMR samples were synthesized as follows. To a solution of $Fe(CO)_3(R^1N{=}C(R^2){-}C(R^3){=}O)$ (**1a**,**b**) (0.25 mmol) in 20 mL of pentane was added 0.9 equiv of DPPE, and the mixture was stirred for 24 h. The resulting voluminous blue precipitate was washed three times with 15 mL of pentane, yielding **7ao**,**bo** in approximately 60% yield as blue powders. The powder was transferred in a NMR tube and cooled to −30 °C, whereupon 0.5 mL of cold (−30 °C) acetone-d_6 was added.

^{31}P NMR and IR Measurement of Complexes 7bl,bn. To a weighted amount of **1b** in a NMR tube at −78 °C was added an equimolar amount of $P(^nPr)_3$ (**n**), or 2 equiv of PPh_3 (**l**) in 0.5 mL of acetone-d_6. The reaction was followed by ^{31}P NMR. After the reaction was completed the solution was evaporated to dryness and the IR was measured.

Elemental Analyses and Mass Spectrometry of Complexes 7. Elemental analyses of complexes **7** were not possible because the obtained solutions were not analytically pure and they did not crystallize. Unfortunately, also the mass spectra could not be obtained due to the extreme sensitivity to air.

Experimental details for the following general procedures for the formation of complexes **8** are given in Table 1.

Synthesis of Bicyclo[2.2.1] Complexes 8akv, 8bkv, 8akkv, and 8bkkv. The reaction of $Fe(CO)_2(P(OMe)_3)({}^t$BuN=C(H)−C(Ph)=O) (**7ak**) with DMAD (**v**) is described as an example. A solution of 1.00 mmol **7ak** in 40 mL of pentane/THF (3:1) was cooled to the appropriate temperature (cf. Table 1), whereupon a solution of 136 μL (1.1 mmol) of DMAD in 20 mL of pentane/THF (1:1) was added dropwise during 30 min. The resulting yellow-brown reaction mixture was evaporated to dryness, and the crude product was purified by column chromatography on silica gel. The reaction with **7bk** was performed analogously. Elution with pentane/Et_2O (1:1) gave a dark brown fraction containing impurities. Subsequent elution with Et_2O/CH_2Cl_2 (9:1) afforded a yellow fraction, which after evaporation of the solvent gave a mixture of **8akv** and **8akkv** as a yellow powder in a total yield of about 60%. The ratio of **8akv**:**8akkv** was approximately 4:1, and in the case of the reaction of **7bk** approximately 7:1 (**8bkv**:**8bkkv**). Pure complexes **8akkv**,**bkkv** could be obtained by stirring a mixture of **8akv**,**bkv** at room temperature in THF with 1 equiv of $P(OMe)_3$. The reaction was followed by IR spectroscopy. Complete conversion to **8akkv**,**bkkv** took ca. 2 and 4 h, respectively. The crude product was purified by column chromatography on silica gel (see Table 1). When the substitution reaction **7a**,**b** → **7ak**,**bk** was performed with 2 equiv of $P(OMe)_3$, the crude reaction mixture was, after cycloaddition,

Table 1. Synthesis of Complexes 8akv,alv,amv,anv, 8aov−x, 8bkv,bmv,bov, and 8akkv,bkkv

complex	reaction temp (°C)	elution ratio[a]	color of the fraction/complex	yield (%)	crystallization[b]
8akv	−80	9:1	yellow	42[c]	pentane/Et_2O
8akkv	−80	9:1	yellow	61[d]	pentane/Et_2O
8alv[e]	−80	CH_2Cl_2	yellow	48	Et_2O/CH_2Cl_2
8amv	−80	9:1	yellow	61	pentane/Et_2O
8anv	−80	9:1	yellow	63	pentane/Et_2O
8aov	−80	Et_2O	yellow/orange	76	*f*
8aow	−30	Et_2O	orange/yellow	73	Et_2O/CH_2Cl_2
8aox[g]	RT	h	orange	43	pentane
8aoy[g]	RT	9:1	red/brown	77	Et_2O/CH_2Cl_2
8bkv	−40	9:1	yellow	52[c]	Et_2O/CH_2Cl_2
8bkkv	−40	9:1	yellow	63[d]	Et_2O/CH_2Cl_2
8bmv	−40	9:1	yellow	62	Et_2O/CH_2Cl_2
8bov	−40	2:1	yellow/green	69	Et_2O/CH_2Cl_2

[a] Ratio of Et_2O/CH_2Cl_2 for elution of **8**. [b] Solvent(s) from which the respective complex is crystallized. [c] Yield when reacted with 1 equiv of $P(OMe)_3$. [d] Yield when reacted with 2 equiv of $P(OMe)_3$. [e] Formed as two isomers. [f] Crystals of **8aov** are obtained by diffusion of pentane in a concentrated CH_2Cl_2 solution of **8aov** at room temperature. [g] The dipolarophile (1.3 equiv) is added in one lot and the reaction mixture stirred at room temperature until complete conversion of the starting complex is reached. [h] Complex **8aox** is eluted with pentane/Et_2O (2:1).

(15) Fe_2CO_9 was prepared by a slightly modified literature procedure, using a quartz Schlenk tube and starting with 25 mL of $Fe(CO)_5$, 150 mL of glacial acetic acid, and 10 mL of acetic anhydride. The latter was added to prevent the mixture from containing too much water. A Rayonet RS photochemical reactor (λ_{max} = 2500 Å) was used for irradiation, and a continuous stream of air was used to cool the reaction mixture. Filtration, washing with water, ethanol, and ether, and subsequently drying in vacuo gave Fe_2CO_9 in usually more than 90% yield: Braye, E. H., Hübel, W. *Inorg. Synth.* **1966**, *8*, 178.

(16) Siebenlist, R.; Frühauf, H.-W.; Vrieze, K.; Smeets, W. J. J.; Spek, A. L. *Eur. J. Inorg. Chem.* **2000**, 907−919.

stirred at room temperature for 2 and 4 h, respectively. Crystalline samples of **8akkv**,**bkkv** were obtained by slow addition of Et_2O to a suspension of **8akkv**,**bkkv** in pentane, followed by cooling to −30 °C for several days.

Synthesis of the Bicyclo[2.2.1] Complexes 8alv,-akv,amv,anv, 8aov−y, and 8bmv,bov. The reaction of $Fe(CO)_2(PEt_3)(^tBuN{=}C(H)\text{-}C(Ph){=}O)$ (**7am**) with DMAD is described as a typical example. A solution of 1.00 mmol of **7am** in 40 mL of pentane/THF (3:1) was cooled to the appropriate temperature (cf. Table 1), whereupon a solution of 136 μL (1.1 mmol) of DMAD in 20 mL of pentane/THF (1:1) was added dropwise during 30 min. The resulting yellow-brown reaction mixture was evaporated to dryness, and the crude product was purified by column chromatography on silica gel. The other reactions were performed analogously, except for the reactions with the less activated dipolarophiles **w**−**y** (cf. Table 1 for details). Elution with pentane/Et_2O (1:1) gave a dark brown fraction containing impurities. Subsequent elution with Et_2O/CH_2Cl_2 (10:1) afforded a yellow fraction, which after evaporation of the solvent gave **8amv** as a yellow powder. The other complexes were chromatographed analogously, except for **8aox** (cf. Table 1). Crystalline samples of **8alv**−**anv, 8aov**−**y**, **and 8bmv**,**bov** were obtained by slow addition of Et_2O to a suspension of the appropriate complex in pentane, or by slow addition of CH_2Cl_2 to a suspension of the appropriate complex in Et_2O, followed by cooling to −30 or −60 °C for several days (cf. Table 1). Crystals of **8aov** suitable for X-ray diffraction were obtained by diffusion of pentane into a concentrated CH_2Cl_2 solution of **8aov** at room temperature.

Synthesis of the Bicyclo[2.2.1] Complexes 8aoz. To a solution of 1.00 mmol of **7ao** in 40 mL of pentane/THF (3:1) at room temperature was added 2 equiv of dimethyl maleate (DMM)[1] in one lot. IR monitoring revealed that the reaction started instantly but did not reach completion. Addition of ca. 20 equiv of DMM resulted in complete conversion to **8aoz**. When the reaction was carried out at −20 °C, complete conversion was reached with 3 equiv of DMM. Upon warming the reaction mixture to room temperature it became deep blue, indicating the formation of the starting complex **7ao**, and an equilibrium between **7ao** and **8aoz** was reached. During workup on silica gel **8aoz** totally decomposed, and thus **8aoz** could not be isolated in this way. Addition of pentane to the cold reaction mixture (−30 °C) resulted in precipitation of **8aoz** (IR). However, even after several washings with pentane/Et_2O (1:1) the precipitate still contained paramagnetic species, which made characterization by NMR spectroscopy impossible.

Preparation of ^{13}CO-Enriched $Fe(CO)_3(MeN{=}C(Ph)$−$C(Ph){=}O)$ (7b). A pentane solution of **7b** (1.00 mmol, 30 mL) was stirred at room temperature for 24 h in a sealed tube (200 mL) under an atmosphere of ^{13}CO. The enrichment was estimated to be about 25% on the basis of IR spectroscopy. The ^{13}CO-enriched **7b** was used to follow the rearrangement reaction **8bv** → **10bv** by ^{13}C NMR.

Synthesis of (^{13}CO-Enriched) Bicyclo[2.2.1] Complex 8bv. A solution of 1.00 mmol of $Fe(CO)_3(MeN{=}C(Ph)$−$C(Ph){=}O)$ (**7b**) in 30 mL of pentane was cooled to 0 °C, whereupon a solution of 136 μL (1.1 mmol) of DMAD in 20 mL of pentane/Et_2O (3:1) was added dropwise during ca. 30 min. The resulting beige precipitate was washed three times with pentane and dried in vacuo, yielding **8bv** as a beige powder in 90% yield.

Synthesis of $Fe(CO)_3$(butenolide) (10bv). (a) A solution of **8bv** (200 mg, 0.039 mmol) in 20 mL of THF was stirred under an atmosphere of CO at room temperature. The reaction was followed by IR spectroscopy. Complete conversion of the starting complex **8bv** to the butenolide **10bv** took approximately 3 h. The resulting yellow-brown reaction mixture was evaporated to dryness, and the crude product was purified by column chromatography on silica gel. Elution with Et_2O/CH_2Cl_2 (3:1) afforded a yellow-brown fraction, which after evaporation of the solvent gave **10bv** as a yellow-brown powder in about 75% yield.

(b) To a solution of 1.00 mmol of $Fe(CO)_3(MeN{=}C(Ph)$−$C(Ph){=}O)$ (**7b**) in 40 mL of pentane/THF (3:1) was added dropwise a solution of 136 μL (1.1 mmol) of DMAD in 20 mL of pentane/THF (3:1) during ca. 30 min under an atmosphere of CO. After all the DMAD was added the reaction mixture was stirred for another 2 h and then chromatographed as described under method a, giving **10bv** in 75% yield.

NMR Study of the Rearrangement of (^{13}CO-Enriched) 8bv to 10bv. A solution of 10 mg of **8bv** in 0.5 mL of $CDCl_3$ at −50 °C was transferred to an NMR tube under an atmosphere of (^{13}CO) carbon monoxide. Immediately a ^{1}H spectrum was recorded which revealed that **8bv** was the only complex present. Upon warming to room temperature, **8bv** starts to isomerize to the corresponding $Fe(CO)_3$(butenolide) complex (**10bv**). During the isomerization the bicyclo[2.2.2] intermediate **9bv** was not detectable by ^{1}H and ^{13}C NMR.

Synthesis of $Fe(CO)_2(PR_3)$(butenolide) (R = OMe, Ph) (10akv,alv). A solution of 1.00 mmol of **7ak** in 40 mL of pentane/THF (3:1) was cooled to −40 °C, and 1 equiv of $P(OMe)_3$ was added, directly followed by the dropwise addition of a solution of 136 μL (1.1 mmol) of DMAD in 20 mL of pentane/THF (3:1) during ca. 30 min. The resulting yellow-brown reaction mixture was evaporated to dryness and the crude product purified by column chromatography on silica gel. Elution with Et_2O afforded an orange fraction, which after evaporation of the solvent gave **10akv** as a yellow-orange powder in about 35% yield. Complex **10akv** was formed as three non-interconverting isomers in a ratio of 20:14:1. The reaction with PPh_3 was performed analogously. The IR revealed that the butenolide complex **10alv** was formed in about 12% yield. The reaction mixture was evaporated to dryness and was washed three times with pentane/Et_2O (2:1). The product was not further purified, and the spectroscopic data were obtained from the raw product. Complex **10alv** was formed as two isomers in a ratio of 9:1.

Reaction of the Bicyclo[2.2.1] Complex 8bv with PEt_3. To a solution of **8bv** (200 mg, 0.039 mmol) in 20 mL of CH_2Cl_2 at −50 °C was added 1 equiv of PEt_3. The reaction mixture was allowed to warm to room temperature, and the reaction was followed by IR spectroscopy. Complete conversion of the starting complex took approximately 3 h. The IR revealed that two products were formed. The main product was $Fe(CO)_2(PEt_3)$(butenolide) (**10bmv**), which was formed in about 30% yield. As second product **8bmv** was formed (IR and ^{31}P NMR) in about 5% yield by substitution of CO for PEt_3 in **8bv**. The reaction mixture was evaporated to dryness and was washed three times with pentane/Et_2O (2:1). The product was not further purified, and the spectroscopic data were obtained from the raw products.

Synthesis of 11a. A weighted amount of complexes **8akv**−**amv** was dissolved in THF and stirred at room temperature under an atmosphere of CO or N_2. The reaction was followed by IR spectroscopy. Complete decomposition of the starting complexes took in both cases between 24 and 48 h, depending on the PR_3 ligand. The reaction mixture was evaporated to dryness and the crude organic product was purified by column chromatography on silica gel. Elution with pentane/Et_2O (1:2) afforded a pale yellow fraction, which after evaporation of the solvent gave **11a** as a yellow oil in about 25% yield. In the case of **8aov**, complete decomposition took approximately 10 days at room temperature and after workup on silica gel gave **11a** in about 15% yield.

Crystal Structure Determination of 8aov. A transparent orange block-shaped crystal was mounted on top of a glass-fiber and transferred to the cold nitrogen stream of an Enraf-Nonius CAD4T diffractometer for data collection at 150 K [rotating anode, 50 kV, 100 mA, graphite-monochromated Mo Kα radiation]. Unit cell parameters were determined from a least squares treatment of the SET4 setting angles of 25

Table 2. Crystal Data and Details of the Structure Determination of 8aov

	8aov		8aov
Crystal Data		Data Collection	
formula	$C_{45}H_{45}FeNO_6P_2$	temperature (K)	150
molecular weight	813.61	θ_{Min}, θ_{Max} (deg)	1.6, 25.00
cryst syst	monoclinic	wavelength (Mo Kα) (Å)	0.71073 (monochr.)
space group	$P2_1/c$ (No. 14)	scan type	ω
a (Å)	11.5238(7)	$\Delta\omega$ (deg)	0.50 + 0.35 tan θ
b (Å)	23.0239(15)	X-ray exposure time (h)	12
c (Å)	18.7570(9)	linear decay (%)	0.7
β (deg)	125.76(1)	dataset	−13:13, 0:27, −13:22
V (Å^3)	4038.3(5)	total data	7395
Z	4	total unique data	7114
D_{calc} (g/cm^3)	1.338	obsd data ($I>2\sigma(I)$)	3857
F(000)	1704		
μ (cm^{-1}) [Mo Kα]	5.02		
crystal size (mm)	0.15 × 0.30 × 0.50		
Refinement			
no. of refined params	501		
final R1	0.069		
final wR2	0.136		
goodness of fit	0.94		
w^{-1}	$\sigma^2(F_o^2) + (0.0438P)^2$		
$(\Delta/\sigma)_{av}$, $(\Delta/\sigma)_{max}$	0.01, 0.00		
min. and max. resd dens (e/Å^3)	−0.40, 0.51		

reflections with 9.96° < θ < 13.82°. The unit cell parameters were checked for the presence of higher lattice symmetry.[17] A total of 7395 reflections were collected and merged into a unique data set of 7114 reflections. Data were corrected for *Lp* but not for absorption. The structure was solved with direct methods (SHELXS86)[18] and subsequent difference Fourier analyses. Refinement on F^2 was carried out by full matrix least squares techniques. H atoms were introduced on calculated positions and included in the refinement riding on their carrier atoms. All non-hydrogen atoms were refined with anisotropic thermal parameters; H atoms with isotropic thermal parameters were related to U_{eq} of their carrier atoms. Weights were introduced in the final refinement cycles. The monoclinic unit cell contains two solvent accessible voids of 55 Å^3 each around inversion centers. No significant residual density was found in that region.

Crystal data and numerical details of the structure determination are given in Table 2. Scattering factors and anomalous dispersion corrections were taken from the International Tables for Crystallography.[19] All calculations were performed with SHELXL97[20] and the PLATON[21] package (geometrical calculations and illustrations). A CIF-file has been deposited with the CCDC: #189587.

Results and Discussion

The complexes discussed in this paper are shown in Schemes 2−6. The type of complexes is identified by Arabic numbers. The two α-iminoketone ligands are differentiated by the letters **a** and **b**. The phosphorus ligands are denoted by the letters **k**−**o** [$P(OMe)_3$ (**k**), PPh_3 (**l**), PEt_3 (**m**), $P(^nPr)_3$ (**n**), and DPPE (**o**)], and the dipolarophiles by the letters **v**−**z** [dimethyl acetylene dicarboxylate (DMAD) (**v**), methyl propynoate (MP) (**w**), phenyl acetylene (**x**), *p*-methoxyphenyl-isothiocyanate (**y**), and dimethyl maleate (DMM) (**z**)]. The α-iminoketone ligands are abbreviated in the text as imket.

Scheme 2. Formation of $Fe(CO)_2(PR_3)$(imket) (7a,bk−n) and Fe(CO)(DPPE)(imket) (7a,bo)

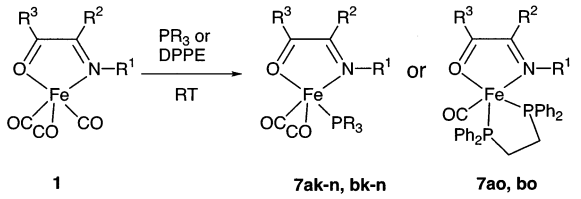

a: R^1= ^{t}Bu, R^2= H, R^3= Ph
b: R^1= Me, R^2= Ph, R^3= Ph

k: R= OMe
l: R= Ph
m: R= Et
n: R= ^{n}Pr
o: $Ph_2PCH_2CH_2PPh_2$ = DPPE

Synthesis of $Fe(CO)_2(PR_3)$(imket) and Fe(CO)(DPPE)(imket) (7). The complexes $Fe(CO)_2(PR_3)$(imket) (**7ak**−**n**,**bk**,**bm**) and Fe(CO)(DPPE)(imket) (**7ao**,**bo**) are prepared via substitution of one or two CO ligands by the respective phosphorus ligand in $Fe(CO)_3$(imket) (**1**) at room temperature (cf. Scheme 2). The reactions are followed by IR spectroscopy. In the case of the relatively small basic phosphines, PEt_3 and $P(^nPr)_3$, the substitution is fast and completed within 10 min with exclusive formation of the monosubstituted complexes. Reactions with the less basic $P(OMe)_3$ and also the more bulky PPh_3 take longer reaction times of 16 and 36 h, respectively. With 2 equiv of phosphorus ligand present these reaction times are reduced to 4 and 12 h. However, in the case of $P(OMe)_3$, the appearance of a CO stretching band at 1917 cm^{-1} indicates that ±10% of the disubstituted product $Fe(CO)[P(OMe)_3]_2$(imket) is also formed.

With the very bulky P^cHex_3 no CO substitution is observed. When **1a** is reacted with 2 equiv of $P(OMe)_3$, PEt_3, or $P(^nPr)_3$, approximately 30% disubstitution has occurred after 2 days. Complete conversion to the disubstituted $Fe(CO)(PR_3)$(imket) complexes requires 10 equiv of PR_3. However, on basis of the intensity of the CO stretching bands in the IR, extensive decomposition has taken place. The Fe(CO)(DPPE)(imket) (**7ao**,**bo**) complexes are prepared by reaction of **1a**,**b** with DPPE in pentane/THF (2:1). IR monitoring indicated that the substitution of the two CO ligands is completed within

(17) Spek, A. L. J. *Appl. Crystallogr.* **1988**, 578.
(18) Sheldrick, G. M. *SHELXS86, Program for crystal structure determination*; University of Göttingen: Göttingen, Germany, 1986.
(19) Wilson, A. J. C. *International Tables for Crystallography*; Kluwer Academic Publishers: Dordrecht, The Netherlands, 1992; Vol. C.
(20) Sheldrick, G. M. *SHELXL97*; University of Göttingen: Göttingen, Germany, 1997.
(21) Spek, A. L. *Acta Crystallogr.* **1990**, *A46*, C-34.

Scheme 3. Observed Reactions of Complexes 1b, 7ak−o, and 7bk−o with the Dipolarophiles v−y

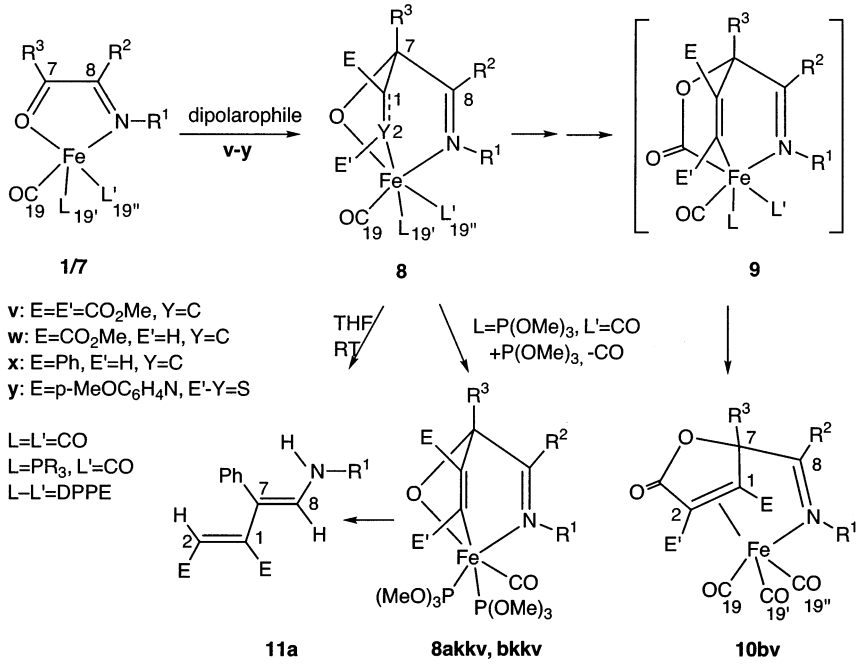

Scheme 4. Reversible Cycloaddition of Fe(CO)(DPPE(ᵗBuN═C(H)−C(Ph)═O) (7ao) with DMM (z)

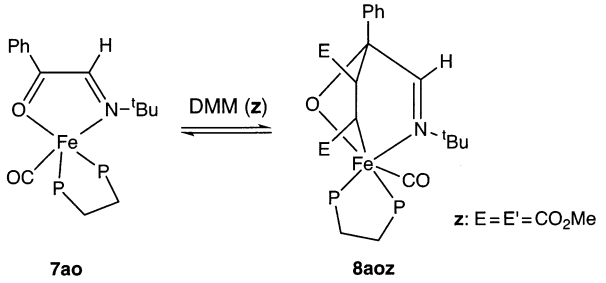

4 h, and the formation of the $Fe(CO)_2$(DPPE)(imket) intermediate with a η^1-coordinated DPPE ligand is not detected. Reaction in pentane takes 16 h due to the limited solubility of DPPE in pentane. In all cases, the substitution is irreversible. Reaction of complexes **7** under CO (1 bar) for 2 days does not lead to any reformation of the starting complexes **1**. Complexes **7** are extremely sensitive to oxygen and moisture. Their structures have been assigned on basis of their IR, UV−vis, and NMR (^{1}H, ^{13}C, and ^{31}P) spectroscopic properties.

Synthesis of the Bicyclo[2.2.1] Complexes (8) and the Butenolide Complexes (10). The 1,3-dipolar cycloaddition reactions of all complexes **7** with DMAD and in the case of **7ao** also with some other dipolarophiles result in the formation of the stable bicyclo[2.2.1] complexes **8**, i.e., the initially formed cycloadduct (cf. Scheme 3). This is surprising because in the reactions of $Fe(CO)_3$(imket) (**1a**) and the analogous $M(CO)_n(CNR)_{3-n}$(R-DAB) (M = Fe; n = 0, 1, 3) and $Fe(CO)_2(P(OMe)_3)$(R-DAB) with DMAD, the initial cycloadduct could never be observed. Even more surprising is the reaction of the tricarbonyl **1b** with DMAD in pentane, which also gives the initial cycloadduct **8bv**. Interestingly, the bicyclo[2.2.1]$Fe(CO)_2(PR_3)$ complexes **8** are obtained as two non-interconverting isomers (cf. NMR section). Complexes **8** have been characterized spectroscopically (IR, ^{1}H, ^{13}C, ^{31}P NMR, FD-mass) and by elemental analyses.

The molecular structure of complexes **8** is established by a single-crystal X-ray structure determination of the bicyclo[2.2.1]Fe(CO)(DPPE) complex **8aov**. In this complex the CO ligand is positioned *trans* to the Fe−O bond, and accordingly insertion of CO into the Fe−O bond cannot take place. However, in the bicyclo[2.2.1]$Fe(CO)_3$ and bicyclo[2.2.1]$Fe(CO)_2(PR_3)$ complexes (**8**) one of the CO ligands is *cis* to the Fe−C bond, which means that insertion of CO is in principle possible. This is indeed found for the $Fe(CO)_3$[2.2.1] bicyclic complex **8bv**. When kept below −30 °C, complex **8bv** is stable in solution under an atmosphere of CO. Above this temperature, however, it reacts further by insertion of CO into the Fe−O bond. Subsequent uptake of an additional CO ligand results in the bicyclo[2.2.2] intermediate **9**, which in turn very rapidly isomerizes (reductive elimination of the two Fe−C bonds followed by recoordination of the double bond) to form the $Fe(CO)_3$(butenolide) complex **10bv**. The reaction **8bv** → **10bv** is followed by NMR. During the conversion the formation of the bicyclo[2.2.2] intermediate **9bv** is not detected, which means that the isomerization **9bv** → **10bv** is fast. Reaction of the bicyclo[2.2.1]$Fe(CO)_2(PR_3)$ complexes **8** in THF or toluene at room temperature under an atmosphere of CO or N_2 results in decomposition, and the formation of the corresponding complexes **10** is not detected. From the decomposition of complexes **8akv**−**anv** in THF the organic compound **11a** is isolated in 25% yield. The DPPE-containing complexes **8** are stable for several days to weeks in THF, but they finally decompose to unidentified compounds. In the case of **8aov** compound **11a** is isolated in 15% yield.

In the case of the reaction with **7ak**,**bk**, the initially formed complexes **8akv**,**bkv** react further with $P(OMe)_3$ that is present in solution to form the corresponding disubstituted complexes **8akkv**,**bkkv**. The additional $P(OMe)_3$ is supplied by partial decomposition. Addition of one extra equivalent of $P(OMe)_3$ results in the

Scheme 5. Reaction of $Fe(CO)_3$(^{t}BuN=C(H)−C(Ph)=O) (1a) with DMAD and PR_3

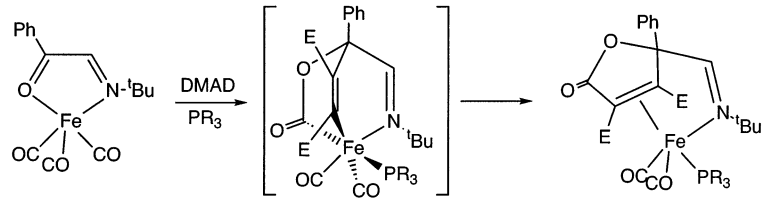

1a **9** **10akv, alv**

E=CO_2Me
R=OMe, Ph

Scheme 6. Reaction of Bicyclo[2.2.1]$Fe(CO)_3$ Complex (8bv) with PEt_3

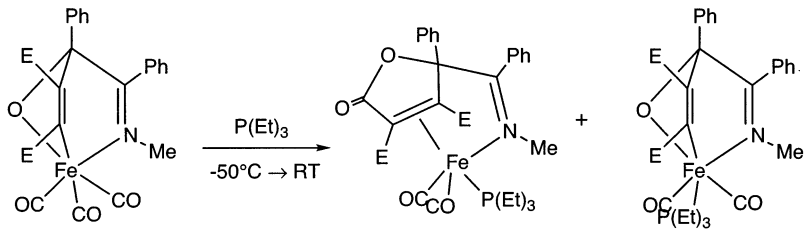

8bv **10bmv** **8bmv**

E=CO_2Me

exclusive formation of **8akkv**,**bkkv**. Reaction of the Fe-$(CO)_2(PR_3)$(imket) complexes **7ak**−**m**,**bk** with MP at −40 °C probably also results in the formation of the initial adducts **8**; however, no identifiable product could be isolated. Complexes **7ak**−**m**,**bk** do not react with the less activated dipolarophiles phenyl acetylene and *p*-methoxyphenyl-isothiocyanate.

With the dipolarophile dimethyl maleate (DMM, **z**), the 1,3-dipolar cycloaddition is reversible (cf. Scheme 4). Complete conversion to **8aoz** at room temperature requires 20 equiv of DMM. At −20 °C, complete conversion to **8aoz** is reached with 3 equiv of DMM. However, upon warming the solution to room temperature the color of the solution became deep blue due to the formation of the starting complex **1ao**, and accordingly **8aoz** could not be purified on silica gel. Unfortunately, complex **8aoz** could also not be characterized after precipitation because the isolated powder still contains, even after repeated washings, small amounts of paramagnetic species, which makes the characterization by NMR spectroscopy impossible.

In the presence of PR_3 (R = OMe, Ph) as an additional ligand, reaction of $Fe(CO)_3$(^{t}BuN=C(H)−C(Ph)=O) (**1a**) with DMAD at −40 °C results in the formation of the corresponding $Fe(CO)_2(PR_3)$(butenolide) complexes (**10akv**,**alv**) (cf. Scheme 5), and the bicyclo[2.2.2] intermediate (**9**) is not observed. Analogous to the reactions with $Fe(CO)_3$(R^1-DAB), the additional PR_3 ligand in intermediate **9** is most probably incorporated exclusively *trans* to the Fe−C(O) bond. However, despite the strengthening effect of the PR_3 σ-donor ligand on the Fe−C(O) bond, it is obviously still very weak and directly reacts further via reductive elimination to form **10akv**,**alv** in low yield. Interestingly, **10akv** is formed as three isomers in a ratio of 20:14:1 and **10blv** as two isomers in a ratio of 9:1 (cf. NMR section). The better stabilizing σ-donor ligand PEt_3 cannot be used in this case because CO substitution is still very fast at −40 °C, resulting in the formation of $Fe(CO)_2(P(Et_3)$(imket).

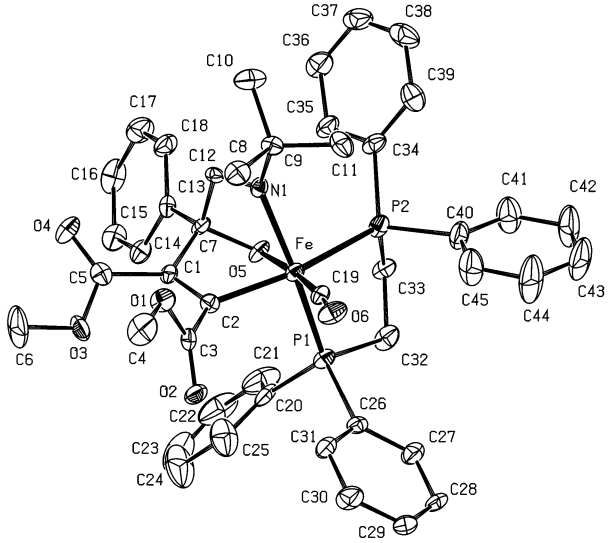

Figure 1. 50% probability displacement ellipsoid plot of **8aov**. Hydrogen atoms are omitted for clarity.

Reaction of **8bv** in the presence of PEt_3 results also in the formation of the $Fe(CO)_2PEt_3$(butenolide) (**10bmv**) in low yield as one isomer, together with traces of **8bmv** (cf. Scheme 6). Complexes **10** have been characterized spectroscopically (IR, ^{1}H NMR, ^{13}C NMR, and ^{31}P NMR) and by elemental analysis of **10bv**.

Molecular Structure of Bicyclo[2.2.1] Complex 8aov. An ORTEP drawing of the molecular structure of **8aov** together with the atomic numbering is shown in Figure 1. Selected bond distances and angles are given in Table 3.

The molecular structure of **8aov** consists of an iron(II) center coordinated by a newly formed [2.2.1] bicyclic structure, in which the iron and the former carbonyl carbon C7 occupy the bridgehead positions, a chelating DPPE ligand, and a CO ligand. The coordination geometry around the central iron atom is strongly

Table 3. Selected Bond Distances (Å) and Angles (deg) for 8aov (SDs in parentheses)

Fe−P1	2.2289(18)	P2−C33	1.814(7)	C1−C5	1.465(7)
Fe−P2	2.2997(16)	O5−C7	1.410(5)	C1−C7	1.537(7)
Fe−O5	1.944(4)	O6−C19	1.154(7)	C2−C3	1.481(7)
Fe−N1	2.025(4)	N1−C8	1.274(7)	C7−C8	1.521(9)
Fe−C2	1.975(5)	N1−C9	1.488(8)	C7−C13	1.492(8)
Fe−C19	1.742(6)	C1−C2	1.354(8)	C32−C33	1.522(7)
P1−C32	1.835(5)				
P1−Fe−P2	85.61(6)	N1−Fe−C2	85.03(18)	Fe−C2−C3	127.0(4)
P1−Fe−O5	83.18(11)	N1−Fe−C19	100.1(2)	C1−C2−C3	121.4(4)
P1−Fe−N1	163.88(15)	C2−Fe−C19	92.1(2)	O5−C7−C1	106.6(4)
P1−Fe−C2	93.84(17)	Fe−C19−O6	174.3(5)	O5−C7−C8	106.0(4)
P1−Fe−C19	96.04(18)	Fe−O5−C7	102.4(3)	O5−C7−C13	109.2(4)
P2−Fe−O5	79.74(11)	Fe−N1−C8	109.5(4)	C1−C7−C8	100.0(4)
P2−Fe−N1	90.58(11)	Fe−N1−C9	129.3(3)	C1−C7−C13	117.5(5)
P2−Fe−C2	162.20(18)	C8−N1−C9	120.6(4)	C8−C7−C13	116.4(4)
P2−Fe−C19	105.69(17)	C2−C1−C5	124.5(4)	N1−C8−C7	114.6(4)
O5−Fe−N1	80.73(17)	C2−C1−C7	112.0(4)	P1−C32−C33	111.0(3)
O5−Fe−C2	82.5(2)	C5−C1−C7	121.3(4)	P2−C33−C32	107.1(4)
O5−Fe−C19	174.5(2)	Fe−C2−C1	109.8(3)		

distorted octahedral. This distortion is a consequence of its [2.2.1] bicyclic structure and the chelating DPPE ligand. The [2.2.1] bicyclic terdentate ligand is not able to span three regular octahedral coordination sites (O5−Fe−N1 = 80.73(17)°, O5−Fe−C2 = 82.5(2)°, and N1−Fe−C2 = 85.03(18)°). These angles are comparable with those of the isostructural [2.2.1] iron[13] (**6**) and ruthenium complex.[7] In addition, the P1−Fe−P2 angle of 85.61(6)° is also smaller than 90° but compares well with the P−Fe−P angles reported in the literature for chelating DPPE ligands.[22−24] The Fe−P1 and Fe−P2 bond distances differ significantly. The rather long Fe−P2 (2.2997(16) Å) distance as compared to the normal Fe−P1 (2.2289(18) Å) distance[22−25] can be explained by the large *trans*-influence of C2, which is known to elongate this bond.[7] The Fe−C2 distance of 1.975(5) Å is somewhat shorter than the comparable Fe−C bond (2.001(4) Å) in the iron [2.2.1] bicyclic structure **6**, which is probably due to the *trans* positioned σ-donor P2, which strengthens the Fe−C2 bond. The intact imine (N1−C8 = 1.274(7) Å) is coordinated to iron by a σ-donative Fe−N1 bond of 2.025(5) Å. As a consequence of the C−C coupling, the former ketone bond C7−O5 is reduced to a single bond, which is reflected in the bond distance of 1.410(5) Å. Furthermore, the central bond of the former alkyne (C1−C2 = 1.354(8) Å) is reduced to a double bond. The olato oxygen O5 is coordinated to iron by a bond of 1.944(4) Å, which compares well with the Fe−O bond length in $Fe_2(CO)_5$-[^{i}PrN═C(H)C(OMe)(O)C(CO_2Me)C(CO_2Me)][26] and Fe_2-$(CO)_6$[CEt═CEt(CO_2)].[27] The rather short Fe−C19 bond of 1.742(6) Å reflects the electron-donating capacity of both the DPPE phosphorus atoms, which enhances π-back-donation to this carbonyl. This is corroborated by the low-frequency position of the CO stretching band in the IR (1910 cm^{-1}) and the high-frequency position of this CO in the ^{13}C NMR (219.7 ppm).

The most important result in the context of this paper, however, is the confirmation of the [2.2.1] bicyclic structure, which proves that the Fe$(CO)_3$(α-iminoketone) complexes react via a mechanism similar to that of the analogous M$(CO)_3$(R^1-DAB) (M = Fe, Ru) complexes.

IR and UV−Vis Spectroscopy. The IR data of the complexes **1**, **7**, **8**, **10**, and compound **11a** are collected in Table 4 (see Supporting Information), together with the elemental analyses, the FD mass, and the UV−vis data.

Complexes 7. The IR spectra of the Fe$(CO)_2(PR_3)$-(imket) (**7ak**−**n**,**bk**−**n**) complexes show two intense CO stretching bands in the ν(CO) region, and the Fe(CO)-(DPPE)(imket) (**7a**,**bo**) complexes give rise to one broad CO stretching band. Compared to the starting Fe$(CO)_3$-(imket) complexes (**1**), the CO stretching bands of complexes **7** are shifted to lower frequency (30−100 cm^{-1}). This is due to the introduction of the strong σ-donating phosphorus ligands as compared to CO, which enhances π-back-donation to the remaining carbonyl(s).

The most pronounced shifts are, as expected, observed for the Fe(CO)(DPPE)(imket) complexes as a result of the substitution of two CO ligands for the two good σ-donor phosphorus atoms of DPPE. The CO stretching frequencies of the monosubstituted Fe$(CO)_2(PR_3)$(imket) complexes nicely parallel the σ-donor capacity[28] (basicity) of the PR_3; that is, the shifts decrease in the order P(^{n}Pr)$_3$ ≈ PEt_3 > PPh_3 > P(OMe)$_3$. Interestingly, in case of the P(OMe)$_3$ complex **7bk**, clearly four bands are seen in the IR, which points to two isomeric forms of **7bk**. The ratio is approximately 1:1. For all other Fe$(CO)_2$-(PR_3)(imket) complexes only two CO bands are observed. Analogously, for Fe$(CO)_2$(2,6-di-^{i}Pr-C_6H_3-DAB)PR_3 (R = OMe)[29] three isomers have been detected, of which two have clearly separated CO bands, while for a series of other PR_3 (R = Ph, c-hex, ^{n}Bu, OPh) ligands only one isomer was observed. The isomeric forms of **7bk** are most probably geometrical isomers of a square pyramidal (sqp) structure because the solid state structure of the starting complex **1b** has approximately this geometry[16] (see NMR section). In the NMR only one set of

(22) Le Narvor, N.; Toupet, L.; Lapinte, C. *J. Am. Chem. Soc.* **1995**, *117*, 7129.
(23) Knorr, M.; Müller, J.; Schubert, U. *Chem. Ber.* **1987**, *120*, 879.
(24) Battaglia, L. P.; Delledonne, D.; Nardelli, M.; Pellizzi, C.; Prediere, G. *J. Organomet. Chem.* **1987**, *330*, 101.
(25) Luh, L.-S.; Liu, L.-K. *Organometallics* **1995**, *14*, 1514.
(26) Siebenlist, R.; de Beurs, M.; Feiken, N.; Frühauf, H.-W.; Vrieze, K.; Kooijman, H.; Veldman, N.; Lakin, M. T.; Spek, A. L. *Organometallics* **2000**, *19*, 3032−3053.
(27) Aime, S.; Milone, L.; Sappa, E.; Tiripicchio, A.; Tiripicchio Camellini, M. *J. Chem. Soc., Dalton Trans.* **1979**, 1155.
(28) Tolman, A. C. *Chem. Rev.* **1977**, *77*, 313.
(29) van Dijk, H. K.; Kok, J. J.; Stufkens, D. J.; Oskam, A. *J. Organomet. Chem.* **1989**, *362*, 163.

resonances is observed, which shows that the geometrical isomers of **7bk** interconvert rapidly on the NMR time scale (10^4 s^{-1}). On the IR time scale (10^{12} s^{-1}), however, the two geometrical isomers of **7bk** can be distinguished. This has also been observed for $Fe(CNR)_3$(^{i}Pr-DAB) (R = ^{t}Bu, c-hex)[4] and $Fe(CO)_3$(η^4-diene).[30] The somewhat lower CO stretching frequencies for complexes **7ak**−**o** compared to those of **7bk**−**o** are due to the better π-accepting properties of α-iminoketone **b**.

The UV−vis spectra of complexes **7** all show an intense absorption band in the visible region between 538 and 599 nm, which unambiguously shows that the α-iminoketone is coordinated in a σ-N, σ-O chelate fashion. The bands are shifted to lower energy compared to those of the parent complexes, and the shifts increase with increasing σ-donor capacity of the phosphorus ligand.

Complexes 8. The IR spectra of complexes **8** show one, two, or three CO stretching bands in the terminal ν(CO) region depending on the number of terminal carbonyls present. As a consequence of the oxidative cycloaddition, the iron is oxidized from Fe(0) to Fe(II) in the [2.2.1] bicyclic complexes **8**, and accordingly the CO stretching bands are shifted ca. 60 cm^{-1} to higher frequency as compared to their precursors **1b** and **7**. Obviously, the lowest CO stretching frequencies are observed for the DPPE-containing complexes **8aov**−**z**,**bov**. Within the DPPE series **8aov**−**x** the CO stretching band shifts to lower frequency as a result of the cycloadded alkyne bearing two, one, and no electron-withdrawing ester groups. The CO stretching bands of **8aoy** and **8aoz** are found at somewhat higher frequency than that of **8aox**, indicating that in both cases the π-back-donation to the remaining carbonyl is reduced. Apparently, the C(sp^3) and S atoms induce less electron density at the iron center than the C(sp^2) carbon in **8aov**−**x**. The CO stretching bands of the mono-PR_3-substituted complexes **8** nicely reflect the basicity of the PR_3 ligand, as those of complexes **7**. The CO stretching bands of the bis-phosphite-substituted complexes **8akkv**,**bkkv** are found at ca. 1945 and 1950 cm^{-1}. This is at approximately 35 cm^{-1} higher wavenumber than in the corresponding DPPE complexes. When the cycloaddition is performed with either DMAD or MP, one broad band of medium intensity is observed in the organic carbonyl region between 1707 and 1694 cm^{-1}. This band is assigned to the carbonyls of the ester substituents. In the case of complex **8aoy**, a band at 1562 cm^{-1} is observed for the C=N double bond of *p*-methoxyphenyl-isothiocyanate, which shows that the C=S bond is cycloadded.

Complexes 10. The three terminal CO ligands of complex **10bv** give rise to an absorption pattern that is characteristic for $Fe(CO)_3$(butenolide) complexes,[5,6,30] i.e., one sharp absorption at higher frequency and two partially resolved absorptions at lower frequency. The CO bands of **10bv** are shifted ca. 35 cm^{-1} to lower frequency compared to those of **8bv** because the iron is reduced from Fe(II) (**8**) to Fe(0) (**10**). As a result of the better π-accepting properties of the α-iminoketone **b**, the CO bands of **10bv** are shifted ca. 10 cm^{-1} to higher frequency compared to those of the earlier reported **10av**.[5] The CO stretching bands of **10ak**,**lv** are observed at 40 cm^{-1} ($P(OMe)_3$) and 50 cm^{-1} (PPh_3) to lower frequency, relative to those of **10av**, due to the introduction of the PR_3 σ-donor ligand. The CO stretching bands of **10bmv** are shifted even further to lower frequency (60 cm^{-1}) compared to those in the corresponding tricarbonyl complex **10bv**, due to the more basic PEt_3 ligand.

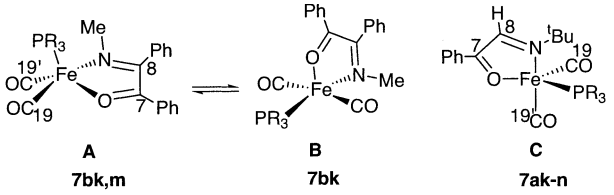

Figure 2. Three different geometries of complexes **7**.

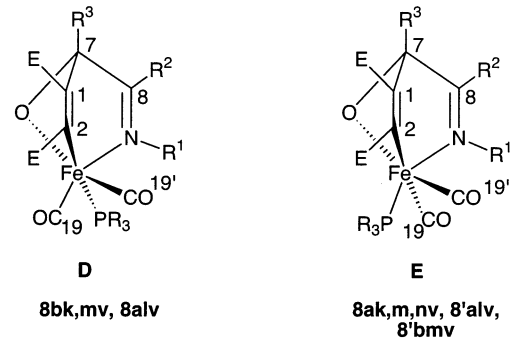

Figure 3. Different ligand arrangements for complexes **8**. Unprimed compound numbers indicate the major (or only) isomer and primed numbers the minor isomer.

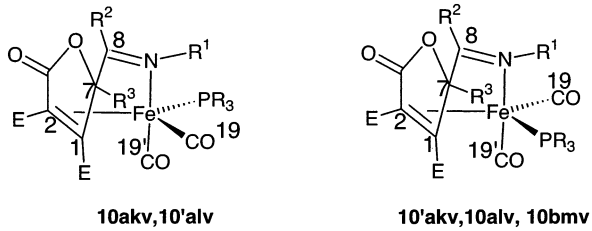

Figure 4. Two isomeric forms of $Fe(CO)_2(PR_3)$(butenolide) (**10**).

NMR Spectroscopy. The ^1H, $^{13}C\{^1H\}$, and $^{31}P\{^1H\}$ NMR data of complexes **1**, **7**, **8**, **10**, and **11a** are collected in Tables 5, 6, and 7, respectively (see Supporting Information). The atomic numbering of selected important proton and carbon atoms is given in Scheme 3 and Figures 2−4.

Complexes 7. The imine proton resonances H(8) in complexes **7al**−**n** are observed as singlets between 8.14 and 8.43 ppm, and in complex **7ak** ($P(OMe)_3$) it is observed as a doublet at 8.84 ppm. These resonances are comparable with that at 8.71 ppm for the $Fe(CO)_3$ precursor **1a**. Only in the case of **7ak** is a small coupling (^4J(P,H) = 2.6 Hz) observed on the imine proton as a result of the larger s-character in the lone pair of $P(OMe)_3$ as compared to the other phosphines, which is known to lead to larger coupling constants.[28] Analogously, all the $P(OMe)_3$-containing complexes **7**, **8**, and **10** also show approximately twice as large P,C coupling constants in the ^{13}C NMR spectra compared to those found for the corresponding PR_3 (R = Ph, Et, ^{n}Pr)-containing complexes. The resonances of the imine C(8)

(30) Angermund, H.; Grevels, F.-W.; Moser, R.; Benn, R.; Krüger, C.; Romão, M. J. *Organometallics* **1988**, *7*, 1994.

and ketone C(7) atoms show coordination shifts of 14−16 and 21−37 ppm, respectively, to lower frequency as a result of extensive π-back-donation from the iron into the low lying π*-orbital of the α-iminoketone. Compared to the resonances of the imine and ketone carbon atoms in the precursor complexes **1a**,**b**, an additional shift of 2−7 ppm (C═N) and 4−12 ppm (C═O) to lower frequency is observed in complexes **7**. The shifts clearly reflect the σ-donor capacity of the phosphorus ligand used; that is, the shifts increase in the order $P(OMe)_3$ < PPh_3, $PEt_3 \approx P(^nPr)_3$ < DPPE. Comparable shifts to lower frequency have been observed for the imine carbon atoms in $Fe(CO)_3(R^1\text{-DAB})$ upon substitution of one[31] or three[4] CO ligands for the more σ-donating/less π-accepting isocyanide ligands. Like in the precursor complexes **1a**,**b**, the larger shifts of the ketone carbon in comparison with the imine carbon atom indicate that the chelate coordination exerts a larger effect on the ketone carbon atom. This may be related to the observed regioselective addition over the Fe−O═C fragment.

As a result of enhanced π-back-donation the resonances of the remaining terminal CO ligand(s) in **7** are shifted to higher frequency. As expected, the shift increases in the order $P(OMe)_3$ < PPh_3, $PEt_3 \approx P(^nPr)_3$ < DPPE, reflecting the σ-donor capacity of the phosphorus ligand. The two terminal CO carbons C(19) and C(19′) in $Fe(CO)_2(PR_3)$(imket) (**7ak**−**n**,**bk**,**bm**) are identical on the NMR time scale down to 193 K; that is, they are observed as one doublet due to coupling with phosphorus. This may be explained by Berry pseudorotations[32,33] which scramble the CO ligands and interchange the two faces of the α-iminoketone ligand. Similar observations have been reported for the CO ligands in $M(CO)_3(R^1\text{-DAB})$ (M = Fe,[34] Ru[35]), $Fe(CO)_2$-$(CNR)(R^1\text{-DAB})$,[31] and $Fe(CO)_3$(α-iminoketone)[5] and for the CNR ligands in $Fe(CNR)_3(R^1\text{-DAB})$.[4]

Interestingly, the ^2J(P,C) coupling constants on C(19) and C(19′) differ significantly between the $Fe(CO)_2(PR_3)$-(imket) complexes **7ak**−**n** and **7bk**,**bm**, respectively. This might indicate that these complexes have different coordination geometries and/or have a different ligand arrangement. This is supported by the difference in the ^{31}P chemical shifts of **7ak**−**n** and **7bk**−**n**. Complexes **7bl** and **7bn** are characterized only by ^{31}P NMR and IR. For complexes **7bk, bm** relatively small P,C coupling constants of 9.1 (**7bm**) and 17.5 Hz (**7bk**) are observed on the terminal carbonyl carbons C(19) and C(19′). In the corresponding complexes **7ak**−**n** these coupling constants are approximately twice as large and lie between 21.8 (**7al**−**n**) and 36.2 Hz (**7ak**). The isostructural $Fe(CO)_2(PR_3)(R^1\text{-DAB})$[36] ($R^1$ = ^{i}Pr, *p*-anisyl) complexes show even smaller P,C coupling constants on the terminal carbonyl carbon atoms which lie between 4.2 Hz (R = Me, Et) and 8.4 Hz (R = OMe). The solid state structure of $Fe(CO)_2(PEt_3)$(*p*-anisyl-DAB) showed that this complex has a square pyramidal (sqp) geometry with PEt_3 coordinated in an apical position and P−Fe−C(O) angles of 80°. Since very small P,C coupling constants are observed on the terminal carbonyl carbons, this geometry is probably preserved in solution. Furthermore, these complexes do not show P,C coupling on the imine carbon atoms. In all complexes **7** a relatively large ^3J(P,C) coupling constant (6−10.6 Hz) on the ketone carbon atom C(7) is found. Only in the case of complexes **7** containing ligand **b** is a ^3J(P,C) coupling (3.8−6.0 Hz) on the imine carbon C(8) observed. A similar effect is found for complexes **8**.

To explain the P,C coupling constants found for complexes **7bk**,**bm**, a distorted sqp geometry is proposed, as shown in Figure 2 (isomer A). The PR_3 is probably somewhat bent away from the N−Fe−O plane, which might explain the rather large ^3J(P,C) coupling on the ketone carbon C(7). Obviously, due to this deformation, also the P−Fe−CO angles change compared to those in $Fe(CO)_2(PEt_3)$(*p*-anisyl-DAB), which results in somewhat larger P,C coupling constants on the terminal carbonyl carbons C(19) and C(19′). It has been shown that **1b** (X-ray)[16] has approximately a square pyramidal geometry (89% along the Berry pseudorotation axes)[37] in which the nitrogen of the α-iminoketone occupies a basal and the oxygen an apical position. The two isomeric forms of **7bk**, seen in the IR, may thus be explained by interconversion between a basal (N)−basal (O) and a basal (N)−apical (O) coordination of the α-iminoketone. However, because on average relatively small coupling constants are found on C(19) and C(19′), the $P(OMe)_3$ is apparently coordinated in a *cis* fashion to both CO ligands (isomer B), i.e., *trans* to the nitrogen σ-donor. This agrees well with the observation that only with the weakest P-donor, $P(OMe)_3$, isomer B is detected.

In complexes **7ak**−**n** significantly larger coupling constants are found on C(19) and C(19′). This may be rationalized by a molecular geometry closely approaching a trigonal bipyramidal (tbp) structure and placing the phosphorus in an equatorial position (cf. Figure 2, isomer C). Because the two CO ligands rapidly interchange positions, the large equatorial coupling constant contributes strongly to the observed averaged value. The change to a tbp structure is in agreement with the decreased π-acceptor capacity of ligand **a** in comparison with that of **b**. From X-ray studies of five-coordinate Fe-(α-diimine) complexes it is known[31,36,38,39] that their geometries change from near tbp to sqp with increasing π-acceptor capacity of the α-diimine.

The coupling constants of **7ao**,**bo** are almost equal, which indicates that they probably have the same ligand arrangement. Interestingly, analogous to the ketone carbon C(7), the carbonyl carbon C(19) in Fe(CO)-(DPPE)(imket) (**7ao**,**bo**) is observed as a triplet due to the coupling with phosphorus. This indicates that the DPPE phosphorus atoms are equivalent, which is confirmed by the singlet observed in the ^{31}P NMR for the two DPPE phosphorus atoms. Since the α-iminoke-

(31) de Lange, P. P. M.; Kraakman, M. J. A.; van Wijnkoop, M.; Frühauf, H.-W.; Vrieze, K.; Smeets, W. J. J.; Spek, A. L. *Inorg. Chim. Acta* **1992**, *196*, 151−160.
(32) Albright, T. A.; Hoffmann, R.; Thibeault, J. C.; Thorn, D. L. *J. Am. Chem. Soc.* **1979**, *101*, 3801.
(33) Berry, R. S. *Chem. Phys.* **1960**, *32*, 933.
(34) Leibfritz, D.; tom Dieck, H. *J. Organomet. Chem.* **1976**, *105*, 255.
(35) Mul, W. P.; Elsevier: C. J.; Frühauf, H.-W.; Vrieze, K.; Pein, I.; Zoutberg, M. C.; Stam, C. H. *Inorg. Chem.* **1990**, *29*, 2336−2345.
(36) Frühauf, H.-W.; Pein, I. Unpublished results, 1988.
(37) Holmes, R. R. In *Progress in Inorganic Chemistry*; Lippard, S. J., Ed.; Wiley: Cambridge, MA, 1984; Vol. 32, pp 119−236.
(38) De Paoli, M. A.; Frühauf, H.-W.; Grevels, F.-W.; Koerner von Gustorf, E. A.; Riemer, W.; Krüger, C. *J. Organomet. Chem.* **1977**, *136*, 219−233.
(39) Kokkes, M.; Stufkens, D. J.; Oskam, A. *J. Chem. Soc., Dalton Trans.* **1983**, 439.

tone ligand is asymmetric, this means that the two phosphorus atoms of DPPE rapidly exchange on the NMR time scale. Unfortunately, variable-temperature ^{31}P NMR experiments (293−193 K) did not change the ^{31}P spectrum; that is, no broadening of the signal was observed. Because two chelating ligands are present in **7ao**,**bo**, the observed exchange cannot be explained by Berry pseudorotations. Therefore a decoordination−rotation−coordination mechanism of one of the chelates must occur to explain the dynamic behavior. As a result of the extra electron density donated by the DPPE ligand, the α-iminoester will be strongly bonded due to extensive π-back-donation into the low lying π*-orbital. Consequently, we assume that one of the phosphorus atoms decoordinates and after rotation coordinates again, thus exchanging the two phosphorus sites. The phosphorus resonances of **7ao**,**bo**, observed at approximately 93 ppm, are shifted exceptionally far (105 ppm) to higher frequency compared to the free ligand (−11.9 ppm). Similar shifts to higher frequency are observed for the isostructural complexes $Fe(CO)_3$(DPPE)[24] and $Fe(CO)(DPPE)(C_4H_6)$,[40] characteristic for five-membered chelate rings.[41,42] Also the resonances of **7al**−**n**,**bl**−**n** are strongly shifted to higher frequency (75−92 ppm) upon coordination, while for **7ak**,**bk** the coordination shift is reduced to approximately 40 ppm. The position of the resonances and the coordination shifts compare very well with those obtained for $Fe(CO)_2(PR_3)(R^1$-DAB).[36]

Complexes 8. In the ^{13}C NMR spectrum of the tricarbonyl complex **8bv** only four resonances are observed that exceed 190 ppm. This indicates that only four carbon atoms are directly bonded to iron. In the related [2.2.2] bicyclic complexes **3** (cf. Scheme 1; X = NR^1, L = L′ = CO) except for these resonances, a fifth signal at 204 ppm is present for the inserted carbonyl. Furthermore, in the mass spectrum of **8bv** a molecular ion peak of 505 mass units is found that corresponds to a 1:1 stoichiometry of **1b** and DMAD. Taken together, this clearly shows that **8bv** has a [2.2.1] bicyclic structure without an inserted CO.

The resonances in the ^{1}H spectrum are observed at their expected positions. The most pronounced changes of chemical shift in the ^{13}C NMR spectrum of **8bv** are observed for the carbon atoms directly involved in the C−C coupling reaction. The resonance of the former ketone carbon atom C(7) is observed at 102.7 ppm, a shift of 78 ppm to lower frequency compared to that in **1d** as a consequence of the change in hybridization from sp^2 to sp^3. The former alkynic carbon C(2) resonates at 154.5 ppm. This is at ca. 25 ppm to higher frequency compared to those in complexes **3** and **6**, which is probably a result of the C−C coupling with a ketone carbon in **8** instead of an imine carbon atom in **3** and **6**. The metal-bonded, sp^2-hybridized, former alkynic carbon C(1) resonates at 192.0 ppm, which compares well with complexes **3** and **6**. The additional shift to high frequency of this carbon atom is caused by the σ-bond to iron, which enhances the carbanionic character of this carbon, resulting in unusually high paramagnetic shielding. The resonance of the intact imine carbon C(8) is shifted ca. 29 ppm to higher frequency in comparison with that in **1b** due to a decrease in π-back-donation to the isolated imine fragment. Similar shifts are found for complexes **3**, **4**, and **6**. The three terminal carbonyl carbon atoms (C(19), C(19′), and C(19″)) give rise to three separate resonances between 206.1 and 201.8 ppm.

The positions of the resonances in the ^{13}C NMR spectra of complexes **8bkv**,**bmv** closely resemble those of **8bv** except for the terminal carbonyl carbons C(19) and C(19′), which are shifted significantly to higher frequency due to the phosphorus σ-donor ligand. The ^{13}C data of **8akv**−**anv** compare very well with those of **8bkv**,**bmv** except for the iron-bonded C(2) resonances which are slightly shifted (9 ppm) to higher frequency and the resonance for the imine carbon C(8) which is shifted ca. 12 ppm to lower frequency due to the substitution of a phenyl for a proton in ligand **a**. The resonances in the ^{1}H NMR are observed at their expected positions.

Interestingly, the bicyclo[2.2.1]$Fe(CO)_2(PR_3)$ complex **8** can form two non-interconverting isomers (cf. Figure 3). This is best to be seen in the reaction of **7ak** with DMAD, which leads to two isomers, **8/8′alv**, in a ratio of 2:1. The major isomer is denoted by its Arabic number, and the minor isomer is primed. These isomers show large differences in their P,C coupling constants, particularly on the iron-bonded carbon C(2). Furthermore, in the ^{31}P NMR two resonances are observed, which differ significantly in their chemical shift (cf. Table 7). Both findings are indicative for coordination of PPh_3 at different coordination sites. The position of PR_3 seems to depend on both the α-iminoketone and the PR_3 ligand. Complexes **8bkv**,**bmv** and **8alv** show large ^2J(P,C) coupling constants (44−68 Hz) on the iron-bonded carbon C(2), which clearly indicates that the PR_3 ligand is positioned *trans* to C(2), a ligand arrangement as shown in Figure 3 (isomer D). On the former ketone carbon C(7) relatively large P,C coupling constants (8.3−10.6 Hz) are found. This coupling information may be conveyed via the C(2)═C(1) bond in *trans*-position to the phosphorus.

In the corresponding complexes **8akv**,**amv**,**anv** and **8′alv** (isomer E), the P,C coupling constants on the iron-bonded carbon C(2) are strongly reduced and lie between 25.7 and 38.5 Hz. Also the coupling constant on the former ketone carbon C(7) is reduced to ca. 3 Hz, and no observable coupling on the imine carbon atom C(8) is observed. In the ^{1}H NMR a very small P,H coupling (<0.7 Hz) on the imine proton H(8) is observed. Superficially, the small couplings suggest that the PR_3 ligand is not in a *trans*-position to nitrogen. This would also avoid two σ-donor atoms, P and N, in mutual *trans*-positions. However, the coordination site *trans* to oxygen is probably even less favorable because the olato oxygen has no π-accepting properties and is also a fairly good donor. The ligand arrangement seen in the solid state structure of **8aov** has one of the P-donors approximately *trans* to C(2) (P(2)−Fe−C(2) = 162.28(18)°) and the other P-donor approximately *trans* to N(1) (P(1)−Fe−N(1) = 163.87(17)°). The latter P-donor in **8aov**, like the P-donor in **8akv**,**amv**,**anv** and **8′alv**, does not couple with imine carbon C(8) and the imine proton H(8). Furthermore the coupling constants on C(2) and

(40) Ungermann, C. B.; Caulton, K. G. *J. Organomet. Chem.* **1975**, *94*, C9.
(41) Garrou, P. E. *Inorg. Chem.* **1975**, *14*, 1435.
(42) Garrou, P. E. *Chem. Rev.* **1981**, *81*, 229.

C(7) in **8aov** are almost similar to those in **8akv**,**amv**,**anv**, and **8′alv**. Consequently, we assume that the PR_3 ligand in the latter complexes is coordinated in a similar position as in **8aov**, i.e., more or less *trans* to nitrogen, as shown in Figure 3 (isomer E). The very small coupling on C(8) and H(8) may indicate that in solution the P(1)−Fe−N(1) angle is smaller than 164° (see above), whereas the P(2)−Fe−C(2) angle is probably more close to 180°, reflected in the large coupling constant on C(2).

In the ^{31}P spectrum of the crude complex **8bmv**, a second resonance was observed at 50.9 ppm (5%) apart from that at 32.4 ppm. Since the ppm value compares well with that found for the corresponding complex **8amv** (52.2 ppm), it probably originates from the isomer (**8′bmv**) with the PEt_3 ligand approximately *trans* to nitrogen.

The preference for one of the two coordination sites, *trans* to C(2) or more or less *trans* to N, probably depends (i) on the steric interactions between the R^1 substituent on the imine nitrogen and the PR_3 ligand and (ii) on electronic factors. From the solid state structure of **8aov** it can be seen that the *tert*-butyl group at N(1) sterically interacts with the coordination site *trans* to C(2). The coordination site *trans* to N(1) is sterically more favorable, although with very bulky PR_3 ligands a steric interaction with the ester at C(2) may be expected. However, this coordination site is thermodynamically less favorable than the coordination site *trans* to the C(2) because it brings the two σ-donors, N an P, approximately in mutual *trans*-positions. With this in mind it is conceivable that for steric reasons complexes **8akv**,**amv**,**anv**, i.e., with the bulky *tert*-butyl group on nitrogen, form the isomer with the PR_3 ligand (R = OMe, Et, ^{n}Pr) in a *trans*-position to nitrogen. With the small methyl group on nitrogen as in complexes **8bkv**,**blv** and **bmv** the coordination site *trans* to C(2) is sterically not hindered and the phosphorus ligand is found exclusively (**8bkv**,**blv**) or preferentially (**8bmv**) in this position. Complex **8blv** was synthesized in a small-scale reaction and is identified by IR and ^{31}P NMR. The position of the phosphorus resonance clearly shows that the isomer with PPh_3 *trans* to C(2) is formed (cf. Table 7). Surprisingly however, in the reaction of **1a** with DMAD and the bulky PPh_3 (**l**) ligand the major of the two formed isomers has the PPh_3 in the sterically less favorable position *trans* to the C(2). With respect to the choice of coordination site for the phosphorus ligand, it can be concluded that a delicate balance exists between (i) the steric interactions of the P-ligand with the substituent on nitrogen and the ester group on C(2) and (ii) electronic factors that disfavor two donor atoms in mutual *trans*-positions.

The DPPE-containing complexes **8aov**−**y**,**bov** give rise to comparable coupling patterns on both the terminal carbonyl carbons C(19) and the iron-bonded carbons C(2). This indicates that these complexes all have the same ligand arrangement, similar to that in the solid state structure of **8aov**. This is supported by the resonances in the ^{31}P spectra, which are found at similar positions. The $^2J(P,P)$ coupling constants of 12.5−34.5 Hz in **8aov**−**y**,**bov** compare well with those reported in the literature.[43,44] The bis-phosphite-substituted complexes **8akkv** and **8bkkv** show similar P,C coupling patterns, which means that they probably have the same ligand arrangement as **8aov**−**y**,**bov**. As expected, significantly larger $^2J(P,P)$ coupling constants are observed (117 and 103 Hz) in these complexes because phosphites give rise to larger coupling constants[28] and the P−Fe−P angle will probably be significantly larger than in the DPPE complexes **8aov**−**y**,**bov**.

For complexes **8aow**−**y** two regioisomeric complexes are possible because the dipolarophiles are asymmetric. It is evident from the ^1H, ^{13}C, and ^{31}P NMR data that in all three cases only one of the isomers is formed. In the case of the *p*-methoxyphenyl-isothiocyanate (**8aoy**) it was shown by the ν(C═N) in the IR spectrum that the C═S bond had reacted. The high-frequency positions of the former alkene protons H(2) (11.43 and 9.67 ppm) in **8aow**,**aox** clearly show that the alkyne carbon atom bearing the proton is bonded to iron, resulting in substantial deshielding. This is in agreement with the high-frequency positions reported by van Wijnkoop et al.[45] and Muller et al.[46,47] for M−C(H)═C proton resonances.

Complexes 10. The ^{13}C NMR data of complex **10bv** compare well with those of the earlier reported closely related complex **10av**.[5] The three carbonyl ligands (C(19), C(19′), and C(19″)) give rise to three separate resonances at somewhat higher frequency in comparison with those of the corresponding **8bv** due to increased π-back-donation as a result of the reduction from Fe(II) (**8**) to Fe(0) (**10**). The most pronounced changes in chemical shift, compared with those in **8bv**, are observed for the two former alkyne carbon atoms C(1) and C(2) which are involved in the isomerization step, i.e., formation of the coordinated butenolide five-membered ring. The alkene carbons C(1) and C(2) in **10bv** resonate at 83.1 and 54.6 ppm, which is within the range normally observed for coordinated alkene carbons. In **10av** they are found at 79.3 and 56.1 ppm, respectively. All other signals are found at their expected positions.

Interestingly, the $Fe(CO)_2(PR_3)$(butenolide) complexes **10** can form three non-interconverting isomers. In the case of $Fe(CO)_2(P(OMe)_3)$(butenolide) three isomers are formed, of which two (**10akv**:**10′akv** = 10:7) are identified by ^1H and ^{13}C NMR. Like for complexes **8**, the major isomer is denoted by its Arabic number and the minor isomer is primed. The third isomer (**10″akv**) could be identified only by ^{31}P NMR because it is formed in low (3%) yield. For PPh_3, two isomers are formed in a ratio of 9:1, of which only the major isomer (**10alv**) is identified by ^1H and ^{13}C NMR. The ^1H and ^{13}C chemical shift positions of **10/10′akv** and **10alv** closely resemble those of **10av** except for the terminal carbonyl C(19) and C(19′) carbon resonances, which experience a considerable shift to higher frequency due to the P-donor. The

(43) Schubert, U.; Gilbert, S.; Knorr, M. *J. Organomet. Chem.* **1993**, *454*, 79.
(44) Coco, S.; Mayor, F. *J. Organomet. Chem.* **1994**, *464*, 215.
(45) van Wijnkoop, M. PhD Thesis, Universiteit van Amsterdam, Amsterdam, The Netherlands, 1992; Chapter 3, pp 71−88.
(46) Muller, F.; van Koten, G.; Vrieze, K.; Heijdenrijk, D. *Inorg. Chim. Acta* **1989**, *158*, 69.
(47) Muller, F.; van Koten, G.; Kraakman, M. J. A.; Vrieze, K.; Zoet, R.; Duineveld, K. A. A.; Heijdenrijk, D.; Stam, C. H.; Zoutberg, M. C. *Organometallics* **1989**, *8*, 982.

P,C coupling constants on C(19) and C(19′) differ significantly in the isomers **10akv** and **10′akv**, indicating a great difference in the P−Fe−CO angles. Also very different P,C coupling constants are observed on the two coordinated alkene carbon atoms C(1) and C(2), respectively. In **10akv** a large coupling is observed on C(1) (32.1 Hz) and a small coupling (6.8 Hz) for C(2), whereas in **10′akv** these coupling constants are reverse, 31.8 Hz on C(2) and 6.8 Hz on C(1). From the solid state structures of $Fe(CO)_3$(butenolide) **10av**[5] it is known that complexes **10** have a trigonal bipyramidal geometry. The observed P,C coupling constants can be explained by the ligand arrangements shown in Figure 4.

An equatorial position of the PR_3 ligands is plausible for electronic reasons because in this way it avoids a *trans* arrangement with the σ-donating imine nitrogen. However, in the case of $P(OMe)_3$ a third resonance is observed in the ^{31}P NMR, which probably originates from the isomer with $P(OMe)_3$ in the *trans*-position to nitrogen. As expected, it is formed in very low yield (3%) and only with $P(OMe)_3$, the weakest σ-donor. In the reaction of **1a** with DMAD and PPh_3, preferentially (90%) the isomer is formed with the PPh_3 ligand *trans* to C(2), while in **10bmv** the PEt_3 ligand is exclusively found in this position. In the cycloaddition of DMAD to $Fe(CO)_3$(α-diimine) with $P(OMe)_3$ as additional ligand, only one example is known where the [2.2.2] bicyclic complex **3** undergoes reductive elimination to form the pyrrolinone complex **4**.[14] (cf. Scheme 1). There, the phosphite ligand is coordinated exclusively *trans* to C(2), which is the thermodynamically most favorable position because C(2) is conjugated with the inserted C=O and thus is a better π-acceptor. Consequently, one would expect that in complexes **10** the PR_3 ligand is coordinated *trans* to C(2). This is found for the PEt_3 ligand in **10bmv** and for the PPh_3 ligand in **10alv**, which is preferentially formed (90%). In the latter case also a small amount of the other equatorial isomer **10′alv** is formed, which might be due to steric interactions of the bulky PPh_3 with the bulky *tert*-butyl group at nitrogen in ligand **a**. In the case of the reaction of **1a** with DMAD and $P(OMe)_3$, the two equatorial isomers are formed in almost equal amounts. Obviously, with the less basic phosphite there is no clear preference for either coordination site.

The observation that the PR_3 ligand in **10bmv**, and less so for **10alv**, ends up in the most favorable position agrees well with the idea of a coordinatively unsaturated intermediate during the rearrangement of **9** → **10**, when the bond between C(2) and the inserted carbonyl carbon has already been formed, but the resulting five-ring has not yet become coordinated via its C(1)=C(2) bond. In this intermediate, the rigidity of **9** is broken and the ligands attached to iron can (pseudo)rotate to their most favorable position before the C(1)=C(2) bond coordinates. This could also explain the low preparative yields for **10**, especially in the case of PPh_3, because bulky substituents hinder recoordination of the double bond and accordingly the coordinatively unsaturated intermediate can decompose via other reaction pathways.

Spectroscopic Characterization and Structural Assignment of 11a. The structure of compound **11a** shown in Scheme 3 is tentatively assigned on the basis of its IR, FD-mass, ^1H NMR, and ^{13}C NMR spectroscopic data. The FD-mass spectrum shows the correct molecular ion peak at 317 mass units. The presence of the new N−H bond in **11a** is confirmed in the IR spectrum by a broad absorption at 3390 cm^{-1}. The two ester carbonyl groups give rise to one broad absorption at 1734 cm^{-1} and a shoulder at 1700 cm^{-1}. In the ^1H NMR the N−H proton is observed as a broad doublet at 4.25 ppm due to the coupling with the former imine proton H(8), which gives rise to a doublet at 6.66 ppm. The large coupling of 13.8 Hz between these two protons indicates that the N−H and C−H bonds are nearly coplanar. Comparable large couplings are observed for the N-protonated butenolide derivatives[26] which are obtained upon decomplexation of the heterocyclic butenolide ligand in **4** (cf. Scheme 1; X = O, R^1 = ^{t}Bu, R^3 = OMe). These compounds possess a similar ^{t}BuN(H)−C(H)=C fragment. The formation of the new double bond is supported by the low-frequency shift of the former imine proton H(8) to 6.66 ppm, a normal position for an alkene proton. Furthermore, both the shift of ca. 27 ppm to lower frequency of the former imine carbon C(8) and the high-frequency shift (42 ppm) of C(7) are indicative of the ^{t}BuN(H)−C(H)=C fragment. The new alkene proton at C(2) is observed as a singlet at 4.93 ppm.

The two hydrogen atoms needed for the formation of **11a** are probably abstracted from THF. Similar proton abstractions[48] from THF have been encountered before in the coordination chemistry of iron carbonyl with α-iminoesters. However, the mechanism is unclear, and because **11a** is a only a side product, no further mechanistic studies were performed.

Formation of Complexes 8 and 10. The product formation in the reactions of **1b** and complexes **7** with the employed dipolarophiles can be explained by the reaction steps depicted in Scheme 3. In the earlier parts[3,7,9,13] of this series we have demonstrated the isolobal analogy[49,50] between the M−N=C fragment (M = Fe, Ru) in $M(CO)_n(CNR)_{3-n}(R^1$-DAB) and an azomethine ylide as a typical representative of a Huisgen 1,3-dipole.[51] Likewise, the Fe−O=C fragment[5,6] in $Fe(CO)_3$(α-iminoketone) is isolobally related to a carbonyl ylide, which is also a well-known organic 1,3-dipole. On this basis, the initial reaction is described as an oxidative 1,3-dipolar cycloaddition of the activated alkynes DMAD and MP across the Fe−O=C fragment, resulting in the bicyclo[2.2.1] intermediate **2** (cf. Scheme 1; X = O). However, it must be noted that the first products that could be characterized and isolated from these earlier reactions were the $Fe(CO)_3$(butenolide) complexes (**4**). The intermediates were proposed on basis of the analogy with the reaction of $M(CO)_n(CNR)_{3-n}(R^1$-DAB) (M = Fe, Ru) with activated alkynes.

The isolation and characterization of the initially formed bicyclo[2.2.1] complexes **8** in the present reactions (cf. Scheme 3) unequivocally proves that the first step is a 1,3-dipolar cycloaddition reaction over the Fe−O=C fragment. Complex **8bv** could be isolated only when the reaction is performed in pentane because it then directly precipitates out of the solution and inser-

(48) Siebenlist, R.; Frühauf, H.-W.; Vrieze, K.; Kooijman, H.; Smeets, W. J. J.; Spek, A. L. *Organometallics* **2000**, *19*, 3016−3031.
(49) Hoffmann, R. *Science* **1981**, *211*, 995.
(50) Hoffmann, R. *Angew. Chem., Int. Ed. Engl.* **1982**, *21*, 711−800.
(51) Huisgen, R. *Angew. Chem.* **1963**, *75*, 604.

tion of CO does not occur. However, in solution above −30 °C **8bv** immediately reacts further by insertion of CO into the Fe−O bond. No matter which additional ligand is offered, CO or PEt_3, the resulting bicyclo[2.2.2] intermediate **9** rapidly isomerizes, via reductive elimination of the two Fe−C bonds followed by recoordination of the double bond, to form the $Fe(CO)_n(PEt_{3-n})$(butenolide) ($n = 0, 1$) complexes **10** (cf. Scheme 6). Analogously, the reaction of **1a** with DMAD and PR_3 (R = OMe, Ph) results in the immediate formation of the corresponding $Fe(CO)_2(PR_3)$(butenolide) complexes **10** (cf. Scheme 5). This means that intermediate **9**, despite the stabilizing P-donor ligand, still rapidly isomerizes. This instability may be attributed to the presence of substituents on the bridgehead carbons of the α-iminoketone, which tend to promote reductive elimination. This was also observed for the reaction of the biacetyl-derived $Fe(CO)_3$-(Np-DAB)[14] with DMAD, where the first observable product is the isomerized pyrrolinone complex (**4**), even when $P(OMe)_3$ is used as additional ligand. Furthermore, the substitution of the more electronegative oxygen in the Fe−C(O)−X fragment instead of NR^1 might weaken the Fe−C(O) bond.

Reactions with Less Activated Dipolarophiles. Reaction of the $Fe(CO)_2(PR_3)$(imket) complexes **7** with the less reactive alkyne MP proceeds readily at −40 °C, which is indicative for the increased reactivity of these complexes. However, no identifiable products can be isolated, which means that the initially formed complexes **8** decompose. Analogously, reaction of $Ru(CO)_3$-(R^1-DAB) results initially in the formation of the bicyclo[2.2.2] $Ru(CO)_3$ adduct at −78 °C. Upon warming, however, it decomposes.[52] A similar type of decomposition could take place in the above-described reactions. The $Fe(CO)_2(PR_3)$(imket) complexes **7** do not react with phenyl acetylene and *p*-methoxyphenyl-isothiocyanate.

Besides with DMAD and MP, the Fe(CO)(DPPE)-(imket) complexes **7ao**,**bo** react also with the less activated dipolarophiles phenyl acetylene and *p*-methoxyphenyl-isothiocyanate to give the corresponding initial adducts **8**. The enhanced 1,3-dipolar reactivity of complexes **7** can be rationalized by electronic arguments. In earlier parts we have shown that in analogy with the organic carbonyl ylide the Fe−O═C fragment can be described as a nucleophilic, HOMO-controlled 1,3-dipole, according to the Sustmann classification.[53−58] This is supported by CAS-SCF calculations.[59−61] It is known that the reactivity of HOMO-controlled cycloadditions is enhanced by the introduction of electron-donating substituents on the dipole. Consequently, the introduction of a PR_3 and especially a DPPE ligand leads to an enhanced 1,3-dipolar reactivity.

Acknowledgment. The investigation was in part supported (W.J.J.S. and A.L.S.) by The Netherlands Foundation for Chemical Research (SON) with financial aid from The Netherlands Organization for Scientific Research (NWO).

Supporting Information Available: Table 4 with IR data, elemental analyses, and mass data, Tables 5−7 with ^1H, ^{13}C, and ^{31}P NMR data. Tables S1−S6 of crystal data and details of structure determination, final coordinates, and equivalent isotropic displacement parameters of the non-hydrogen atoms, Hydrogen atom positions and isotropic displacement parameters, (an)isotropic displacement parameters, and bond distances and angles for compound **8aov**. This material is available free of charge via the Internet at http://pubs.acs.org.

OM020605Z

(52) van Wijnkoop, M. Personal communication.

(53) Sustmann, R. *Tetrahedron Lett.* **1971**, 2721.
(54) Sustmann, R.; Trill, H. *Angew. Chem., Int. Ed. Engl.* **1972**, *11*, 838.
(55) Sustmann, R. *Pure. Appl. Chem.* **1974**, *40*, 569.
(56) Houk, K. N.; Yamaguchi, K. *1,3-Dipolar Cycloaddition Chemistry*; John Wiley and Sons Inc.: New York, 1984.
(57) Fukui, K. *Acc. Chem. Res.* **1971**, *4*, 57.
(58) Herdon, W. C. *Chem. Rev.* **1972**, *72*, 157.
(59) Houk, K. N.; Sims, J.; Duke, R. E.; Strozier, R. W.; George, J. K. *J. Am. Chem. Soc.* **1973**, *95*, 7287.
(60) Houk, K. N. *Acc. Chem. Res.* **1975**, *8*, 361.
(61) Dedieu, A.; Liddel, M. J. Unpublished results.